# SEASONAL REORGANIZATION OF CLIMATE SIMILARITY IN THE CARPATHIAN BASIN: A TIME-BASED CLIMATE NETWORK APPROACH

***Attila MAGYARI-SÁSKA***[1]

DOI: 10.21163/GT_2026.213.12

**ABSTRACT**

This study examines changes in the seasonal organisation of climate in the Carpathian Basin using a time-based climate-network approach. In contrast to conventional climate networks, where nodes usually represent spatial locations, the present method defines individual year–month observations as network nodes. Edges describe multidimensional climatic similarity based on monthly values derived from daily temperature, precipitation, humidity and radiation data. The analysis uses E-OBS gridded observational data for ten selected locations and compares two 30-year periods: 1961–1990 and 1995–2024. The results show that the annual climatic cycle remained broadly recognisable in the recent period, with stable winter and summer components still present in the network structure. However, the boundaries between seasonal groups became less sharply defined. The strongest changes were associated with transition months, especially February, March, April, September and October. Shannon entropy indicates that some of these months became more fragmented, while prototype similarity matrices reveal stronger cross-seasonal relationships between spring and autumn states. Percolation analysis shows only minor changes in overall network robustness, suggesting that the observed transformation should not be interpreted as a collapse of the seasonal structure, but rather as a moderate reorganisation of the relationships between monthly climatic states. The study demonstrates that time-based climate networks can complement conventional trend-based climate analyses by highlighting structural changes in the temporal organisation of seasonality.

***Keywords****: time-based climate networks; seasonal reorganisation; Carpathian Basin; climatic similarity; Shannon entropy; percolation analysis*

## 1. INTRODUCTION

Climate change is usually described through changes in individual climatic variables, such as temperature, precipitation, humidity or radiation (Stine et al., 2009; Stine and Huybers, 2012). These variables are commonly analysed by trends, anomalies, extremes or spatial patterns, and such approaches remain essential for understanding regional climate dynamics. At the same time, climate is not experienced as a set of isolated variables. It is organised through recurring seasonal states, transitions between months, and similarities between different parts of the annual cycle. For this reason, changes in climate may also appear as changes in the internal structure of seasonality: some months may become more similar to others, some transitional periods may become less clearly defined, and the stability of the annual cycle may be modified even when the general seasonal order remains recognisable (Stine et al., 2009; Hajek et al., 2022).

This structural perspective is particularly relevant in regions where several climatic influences meet like in the Carpathian Basin (Spinoni et al., 2015b). Situated between Central and South-Eastern Europe, it is shaped by oceanic, continental and local topographic influences. Its climate is therefore not only spatially heterogeneous, but also strongly seasonal. The basin includes lowland areas, enclosed depressions, hilly regions and mountain-influenced zones, all of which may respond differently to ongoing climatic change.

[1] *Babeș-Bolyai University, Faculty of Mathematics and Computer Science, 400084 Cluj-Napoca, Romania, magyari.saska.attila@gmail.com, attila.magyari@stud.ubbcluj.ro*

Previous research has already shown that the region is sensitive to changes in temperature and precipitation regimes, with consequences for agriculture, water resources and environmental stability (Bartholy and Pongrácz, 2007; Spinoni et al., 2015a; Spinoni et al., 2015b; Jánosi et al., 2023; Megyeri-Korotaj et al., 2023). However, beyond changes in the magnitude of climatic variables, it is also important to ask whether the temporal organisation of the regional climate has changed. Network-based methods offer a useful framework for this type of question (Tsonis and Roebber, 2004; Tsonis et al., 2006; Donges et al., 2009). In climate research, networks are most often used to represent spatial relationships: nodes usually correspond to grid cells or meteorological stations, while edges describe statistical similarity, correlation or coupling between climatic time series (Tsonis and Roebber, 2004; Donges et al., 2009; Holme and Rocha, 2023). Such spatial climate networks have been applied to the study of teleconnections, climate regimes and large-scale atmospheric patterns, including phenomena such as El Niño (Ludescher et al., 2023). This line of research has shown that graph-based representations can reveal structural properties of the climate system that are not always visible through conventional statistical summaries.

The temporal dimension of climate similarity has received less attention (Holme and Saramäki, 2012; Mucha et al., 2010). If spatial climate networks ask how different places are connected through climate behaviour, a time-based climate network asks a different question: how are different time periods connected to each other? From this perspective, months or seasons can be treated as elements of a climatic system (Holme and Saramäki, 2012; Stine et al., 2009). Their relationships can be described by the similarity of their multidimensional climatic conditions. Such an approach is especially suitable for investigating whether the annual cycle has become more fragmented, more internally differentiated, or more strongly reorganised over time.

The study is guided by three main questions. First, can a time-based network representation reveal changes in the seasonal organisation of climate in the Carpathian Basin? Second, which parts of the annual cycle show the strongest structural reorganisation between the two periods? Third, do these changes indicate a general weakening of the climatic network, or rather a reconfiguration of seasonal relationships while the overall annual structure remains stable? By addressing these questions, the paper contributes both to regional climate analysis and to the methodological development of climate-network research. Its regional contribution lies in identifying how the internal seasonal structure of the Carpathian Basin has changed during the last six decades. Its methodological contribution lies in adapting established tools of network analysis, including similarity-based graph construction, community detection, entropy measures and percolation analysis, to a temporal-node framework (Fan et al., 2018). This makes it possible to study climate not only as a spatially connected system, but also as a temporally organised structure.

## 2. STUDY AREA AND DATA

The analysis focuses on the Carpathian Basin, a climatically diverse region situated in Central and South-Eastern Europe. The ten locations were selected using a stratified, purposive design intended to span the principal geographical and climatic contrasts of the basin rather than to constitute a statistically representative sample of all grid cells. Győr and Keszthely represent the western sector of the basin, including more pronounced western atmospheric influences and, in the case of Keszthely, the vicinity of Lake Balaton. Kecskemét represents the open central Pannonian lowland, while Pécs represents the southern foothill zone. Košice and Oradea cover the northern and eastern margins of the Pannonian lowland and its transition toward the surrounding mountain system. Cluj-Napoca and Deva represent Transylvanian hilly and valley environments, whereas Gheorgheni and Brașov represent elevated, enclosed intra-mountain depressions. Together, the selected locations cover open plains, foothill transition zones, hilly and valley environments, and mountain-controlled basins. This design makes it possible to examine whether the inferred changes in seasonal climate-network organisation recur across contrasting regional settings. The study locations should therefore be regarded as physiographically and climatically contrasting case-study sites rather than as an area-weighted sample of the entire Carpathian Basin (Fig. 1).

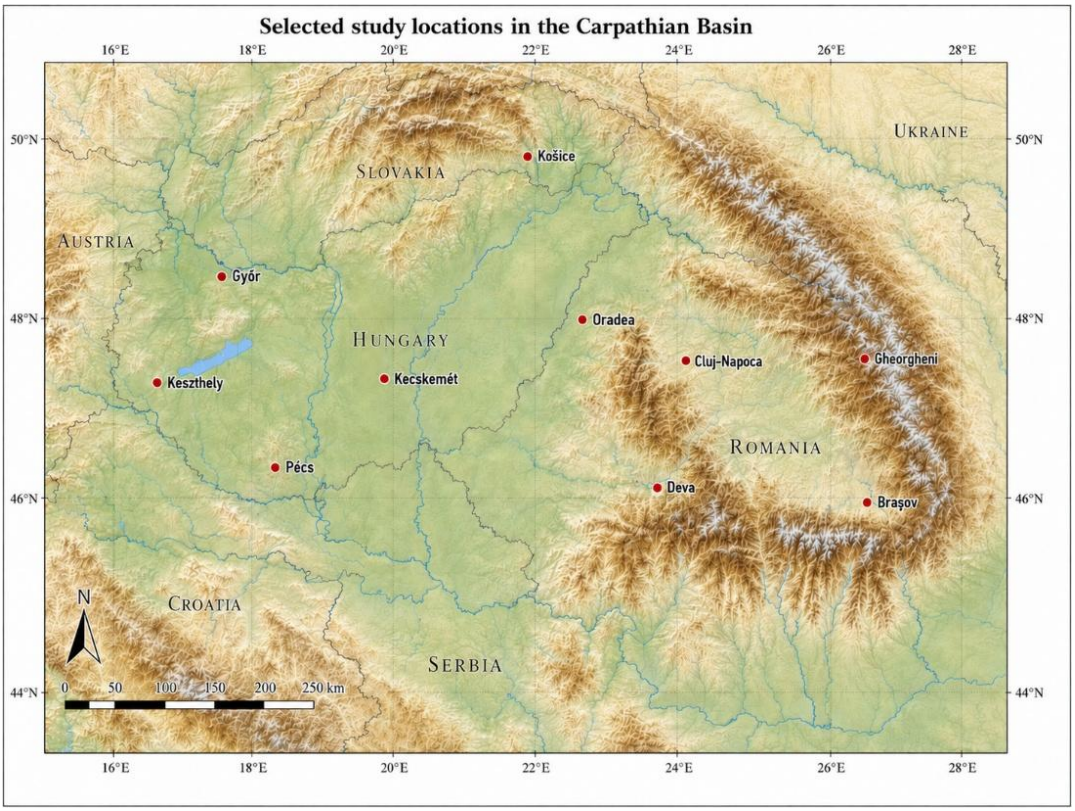


**Fig. 1.** Study locations in the Carpathian Basin

For each location, the corresponding grid cell of the E-OBS gridded observational dataset was used. The analysis was based on the 0.1° × 0.1° regular latitude–longitude grid version 31.0e, obtained from the Copernicus Climate Data Store. The data were obtained from the Copernicus Climate Data Store. E-OBS consists of station-based daily observations spatially interpolated to a regular European grid. Six daily variables were extracted for each selected location: daily mean temperature (TG), daily minimum temperature (TN), daily maximum temperature (TX), daily precipitation sum (RR), daily mean relative humidity (HU) and daily mean global radiation (QQ) to describe each month as a multidimensional climatic state.

Each month in each year therefore became one observation described by a six-dimensional climatic vector. The temporal coverage was divided into two 30-year periods. The early period extends from January 1961 to December 1990, while the late period extends from January 1995 to December 2024. These two intervals were selected to compare a historical baseline with a more recent climatic period of the same length.

## 3. METHODOLOGY

Since the six variables have different units and numerical ranges, the monthly feature vectors were first standardised. This step prevents variables with larger absolute values, such as precipitation totals, from dominating the distance calculation. After standardisation, Principal Component Analysis (PCA) was applied to reduce the six-dimensional space to two dimensions to obtain a compact space in which the main multidimensional differences between months are preserved. Similarity was then calculated from the Euclidean distance between monthly observations in this reduced PCA space. For two nodes ($i$) and ($j$), with projected coordinates ($p_i$) and ($p_j$), the distance was calculated as (Eq. 1):

$$d(i,j) = \sqrt{\left(p_{i,1} - p_{j,1}\right)^2 + \left(p_{i,2} - p_{j,2}\right)^2} \quad (1)$$

The distances were transformed into similarity values using min–max scaling followed by inversion (Eq. 2):

$$S(i,j) = 1 - \frac{d(i,j) - d_{min}}{d_{max} - d_{min}} \quad (2)$$

Thus, a value close to 1 means that two months occupy a very similar position in the reduced climatic space, while lower values indicate more distinct monthly states. For the early and late networks, the same reference scale was used. The minimum and maximum distances used in the transformation were derived from the full available period, so that similarity values in the two networks remained directly comparable.

The pairwise similarity calculation initially produces a complete weighted graph, where each month is connected to all other months. For a meaningful interpretation a pruning step was applied to extract the main structural backbone of the network. All edges were ranked according to their similarity values, and the weakest edges were removed until a predefined average degree was reached. For this, instead of using a fixed similarity threshold, the method therefore keeps network density comparable between locations and periods. The target average degree was defined as (Eq. 3):

$$\langle k \rangle = 3Y - 1 \quad (3)$$

where ($Y$) is the number of years in the analysed period. Since both comparison periods contain 30 years, this gives a target average degree of 89. The corresponding number of retained edges is (Eq. 4):

$$E_{target} = \frac{\langle k \rangle \times N}{2} \quad (4)$$

where ($N$) is the number of nodes in the network. This rule follows the assumption that, under stable seasonal conditions, a month should remain strongly connected to its own calendar-month occurrences in other years and to the neighbouring parts of the annual cycle. The weight of the weakest retained edge defines the empirical structural threshold of the given network.

The community structure analysis aim was to identify groups of month-year observations that form internally coherent climatic blocks. In this context, a community can be interpreted as a set of months that are more similar to each other than to the rest of the annual cycle (Newman, 2006). The Leiden algorithm was used for community detection, with edge weights included in the partitioning process (Traag et al., 2019). The resulting communities were not interpreted only as abstract graph clusters, but they were compared with calendar months in order to see whether the detected structure follows the expected seasonal order, and whether this order changes between the early and late periods. The quality of the detected partition was summarised by modularity, which measures how strongly nodes are grouped within communities compared with the connections expected in a random network. Higher modularity indicates more clearly separated seasonal blocks, while lower modularity indicates weaker separation and stronger overlap between seasonal communities.

To describe how stable or fragmented each calendar month is within the detected communities, Shannon entropy was calculated for every month (Shannon, 1948). For a given calendar month, the distribution of its 30 year–month observations across communities were used. The entropy of month ($m$) was calculated as (Eq. 5):

$$H_m = \sum_{c=1}^{C} p_{m,c} * ln(p_{m,c}) \quad (5)$$

where ($p_{m,c}$) is the proportion of observations of month ($m$) assigned to community ($c$), and ($C$) is the number of communities containing observations from that month. Higher entropy values indicate a more fragmented or transitional monthly position, while lower values indicate a more stable community membership.

Community detection and entropy describe the internal structure of each period separately. To compare the typical position of calendar months between the early and late periods, prototype similarity matrices were also calculated. For each location and each period, a monthly prototype was created for every calendar month, representing the average climatic state of that month over the 30-year period. The early and late prototypes were projected into the same PCA-based reference space used for the network construction. Similarities were then calculated between all early and late monthly prototypes, producing a 12 × 12 matrix.

Percolation analysis was used to describe the robustness of the entire network. The procedure examines how the network breaks apart when weaker edges are progressively removed. For each network, a series of increasing similarity thresholds was applied. At each threshold, only edges with weights equal to or higher than the threshold were kept. The size of the largest connected component was then calculated as a proportion of all nodes. As the threshold increases, the network gradually loses edges and eventually fragments. The critical percolation threshold was defined as the threshold before the largest drop in the size of the largest connected component. This point marks the similarity level at which the network loses a major part of its connectivity. A higher critical threshold means that the network remains connected even when only strong similarities are kept. A lower critical threshold indicates earlier fragmentation. To compare the two periods, a percolation index was calculated as (Eq. 6):

$$I_{perc} = \tau_c^{late} - \tau_c^{early} \quad (6)$$

where ($\tau_c^{early}$) and ($\tau_c^{late}$) are the critical thresholds of the early and late networks. Positive values indicate that the late network is more robust than the early one, while negative values indicate that it fragments at a lower similarity threshold.

## 4. RESULTS

### 4.1. General structure of the time-based climate networks

The comparison of the early and late time-based climate networks shows that the annual climatic cycle did not undergo a complete structural breakdown. In most cases, the detected communities still followed a broad seasonal logic. The networks were usually organised around three main blocks, corresponding to winter, summer and transitional months. In a few cases, a fourth community also appeared, but this did not represent a new stable seasonal regime. It was generally linked to the separation of one or a small number of isolated nodes. The more relevant change was not the number of communities itself, but the way in which these communities became connected to each other. Modularity decreased at all ten selected locations between the early and late periods (**Fig. 2**). This indicates that the seasonal blocks became less sharply separated in the contemporary period. The winter and summer cores remained identifiable, but the boundaries between the main seasonal groups became weaker.

This pattern is important as suggests a reorganisation of the seasonal structure rather than a simple increase or decrease in climatic variability. The annual cycle remained recognisable, but the internal separation between its main components became less clear. The most visible changes were connected

to the months located near seasonal boundaries, especially late winter, spring and early autumn. The community-detection results therefore provide the first indication that the contemporary climate networks are not simply more fragmented in a general sense. Instead, they show a more subtle change: stable seasonal cores are preserved, while the transition zones between them become more flexible and less clearly delimited.

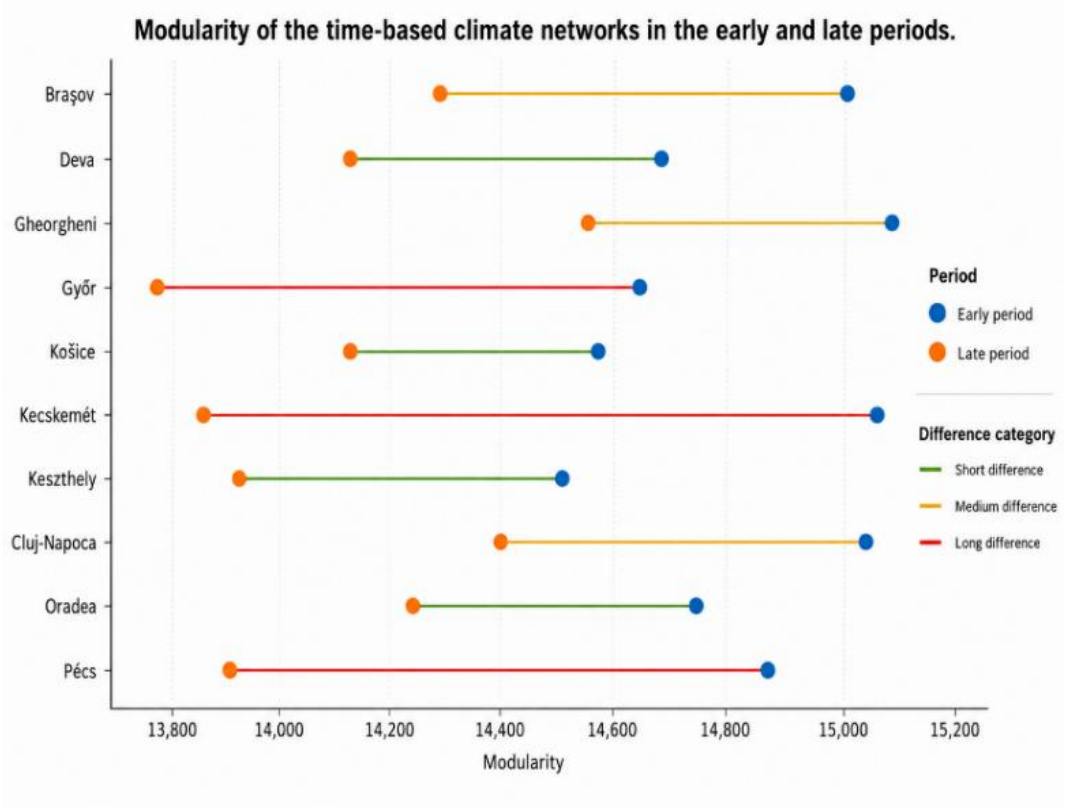


**Fig. 2.** Change in modularity between the early and late periods.

### 4.2. Monthly fragmentation based on Shannon entropy

Shannon entropy was used to describe how clearly the observations of a given calendar month belong to the detected communities. Low values indicate that the month is concentrated in one community, while higher values show that its observations are distributed across several communities. In this sense, entropy measures the stability or ambiguity of monthly community membership.

The monthly averages of the considered locations show that changes were concentrated in specific parts of the annual cycle rather than distributed evenly throughout the year (**Fig. 3**). January and December remained completely stable in both periods, with average entropy values of 0.000. The core summer months also changed only slightly, especially June, July and August. This confirms that the middle of winter and the middle of summer preserved a relatively coherent network position. The strongest changes were instead linked to the transition months.

The clearest increase occurred in February. Its average entropy rose from 0.078 in the early period to 0.328 in the late period, and this increase was visible at nine of the ten locations. The location-level heatmaps confirm that February became more fragmented almost everywhere, with the only exception being Košice, where entropy remained unchanged. This suggests that late winter became less consistently attached to a single winter community and more often shared similarities with transitional climatic states (**Fig. 4**).

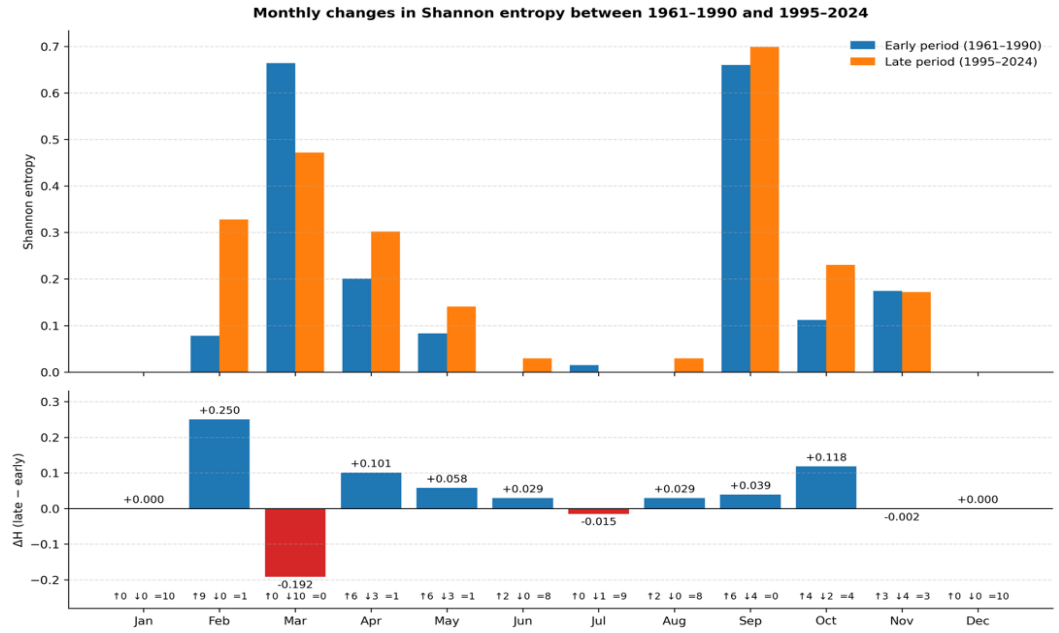


**Fig. 3.** Monthly Shannon entropy in the early and late periods.

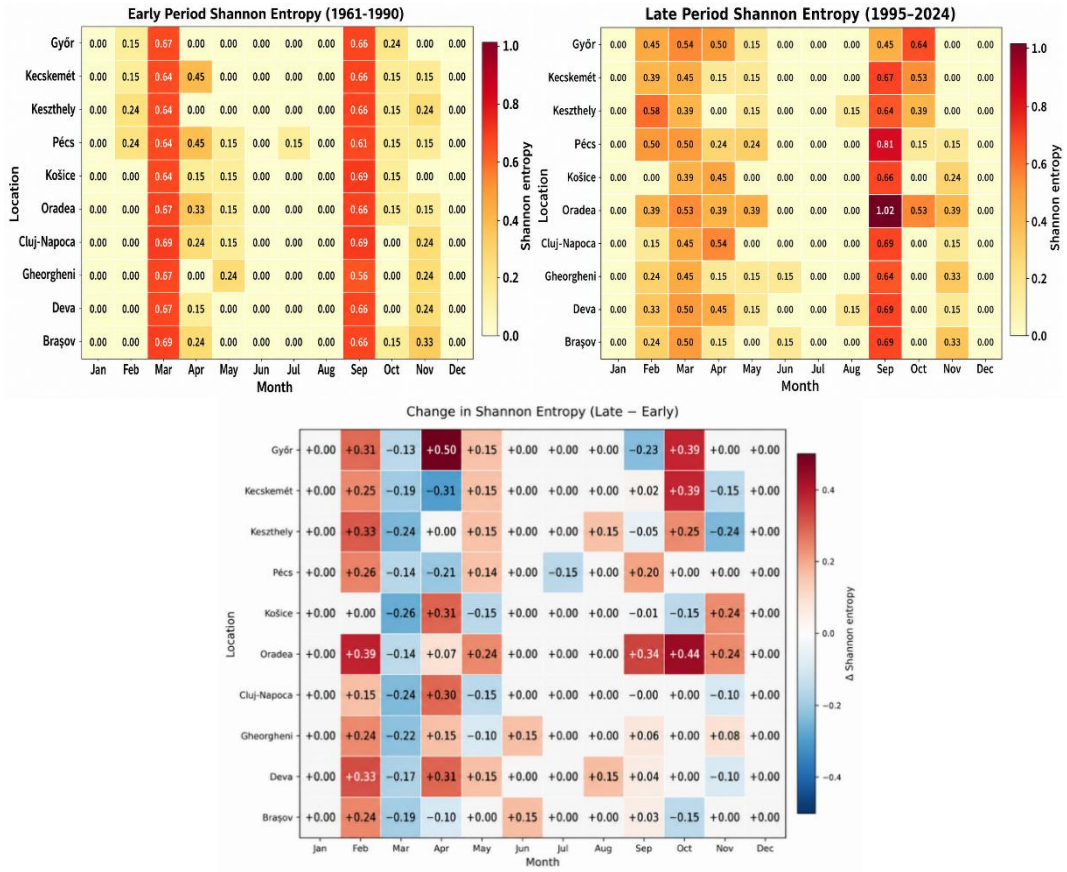


**Fig. 4.** Shannon entropy by location and month between the late and early periods.

March shows the opposite pattern. Its average entropy decreased from 0.664 to 0.472, and the decrease occurred at all selected locations. The heatmaps make this result especially clear: March was one of the most fragmented months in the early period, but its entropy became lower everywhere in the late period. This does not mean that the spring transition disappeared. Rather, it suggests that March became less divided between winter-like and spring-like communities and moved toward a more coherent transitional or early-spring position.

April and May show a more mixed spatial pattern. Their average entropy increased moderately, but the heatmaps reveal that this increase was not uniform across the basin. In April, entropy increased clearly at Győr, Košice, Cluj-Napoca and Deva, while it decreased at Kecskemét, Pécs and Brașov. May also shows both positive and negative changes depending on location. This means that the spring transition did not reorganise in a single regional direction. Instead, it changed through locally different adjustments in the position of individual months.

September remained one of the most complex months in the annual cycle. Its entropy was already high in the early period and remained high in the late period as well. The heatmaps show that September continued to have elevated entropy values at most locations, with particularly high late-period values at Oradea and Pécs. This confirms its persistent transitional character. September does not behave as a stable late-summer or early-autumn month only, but as a climatic boundary zone where different seasonal signals overlap.

October became more fragmented on average, but again with strong spatial differences. The largest increases appear at Győr, Kecskemét, Keszthely and Oradea, while Košice and Brașov show decreases. November remained almost unchanged in the basin-wide average, although the change heatmap shows that this apparent stability hides local contrasts: entropy increased at some locations, such as Košice and Oradea, but decreased at others, including Keszthely, Kecskemét, Cluj-Napoca and Deva.

Overall, the entropy results support the interpretation that the core months of winter and summer remained relatively stable, while the transition months underwent the strongest reorganisation. The annual cycle therefore changed mainly through the restructuring of its seasonal margins rather than through a uniform shift affecting all months equally.

### 4.3. Prototype similarities and cross-seasonal shifts

The prototype similarity matrices provide a direct comparison between the typical monthly climatic states of the early and late periods. They help to identify whether the same calendar months remained close to their earlier climatic position, or whether stronger cross-seasonal similarities appeared.

The general pattern confirms that the main annual structure was preserved. Winter months remained most similar to winter-like late-period states, and the summer months continued to form a clearly recognisable warm-season block. This means that the basic seasonal order did not disappear. The networks do not indicate a collapse of the annual cycle into an undifferentiated structure (**Fig. 6**).

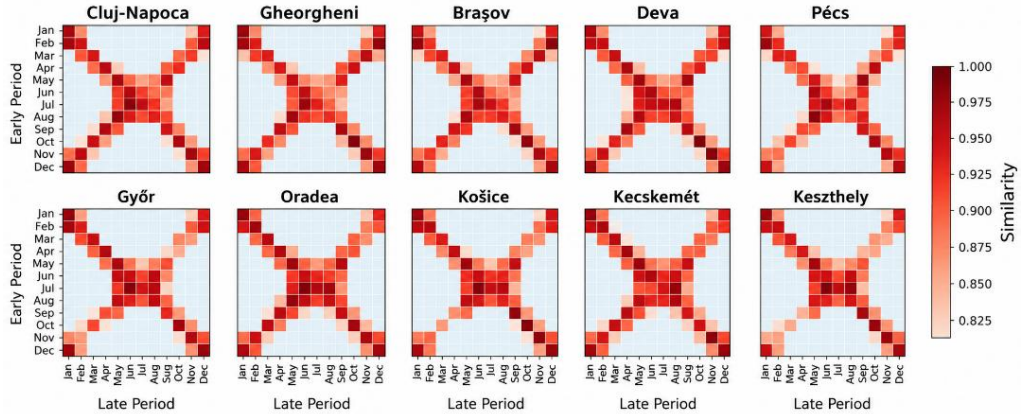


**Fig. 6.** Mean prototype similarity by location.

The most informative changes appear outside the diagonal of the prototype matrices. These off-diagonal similarities show where months from the early period became strongly connected to different months in the late period. After applying the structural thresholds, several spring–autumn and late-summer–autumn overlaps remained visible. This indicates that these similarities were not only weak background relations, but part of the stronger network structure.

The case of Pécs illustrates this pattern clearly (**Fig. 7**). In the thresholded prototype matrix, early April shows a very high similarity to late October, with a value of 0.95. Early May is most strongly linked to late September, with a similarity of 0.97. These values point to a stronger overlap between spring, late-summer and autumn transitional states. The result should not be interpreted as a direct replacement of one month by another, but rather as evidence that the climatic similarity field of transitional months became more interconnected.

Similar patterns also appear at other locations, although with different strength. The thresholded matrices show that even after removing weaker background similarities, the transition periods retain important cross-seasonal links. This is consistent with the entropy results: the largest changes are not located in the stable winter and summer cores, but in the months where seasonal identities are naturally less fixed.

The prototype analysis therefore adds an important layer to the results. Community detection shows that the seasonal blocks became less sharply separated, and Shannon entropy identifies which months became more or less fragmented. The prototype matrices show how this reorganisation appears in terms of direct month-to-month similarity between the two periods.

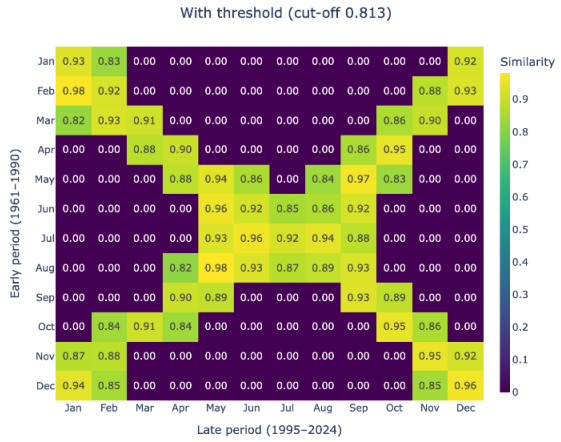


**Fig. 7.** Thresholded prototype similarity matrix of Pécs.

### 4.4. Percolation robustness

Percolation analysis was used to evaluate whether the observed seasonal reorganisation also involved a weakening of the whole network backbone. The percolation indices remained close to zero at the selected locations, indicating only moderate changes in global network robustness.

Across the ten locations, the percolation index ranged from −0.01419 to +0.01002, with an average value of −0.00257. The average direction of change was therefore slightly negative, meaning that the late-period networks tended to fragment at somewhat lower similarity thresholds considering the whole Carpathian Basin.

At the same time, different types of changes in this indicator can be observed at each location and they can be grouped into three broad categories (**Fig. 8**). The first group includes locations with negative percolation indices, where the late-period network became slightly more fragile. This group includes Brașov, Deva, Pécs, Košice, Kecskemét and Cluj-Napoca. The strongest negative shift was found in Brașov (**Fig. 9**), where the index reached −0.01419 and the critical threshold decreased from approximately 0.971 to 0.957. Deva also showed a relatively stronger negative value, while the changes at Košice, Kecskemét and Cluj-Napoca were smaller.

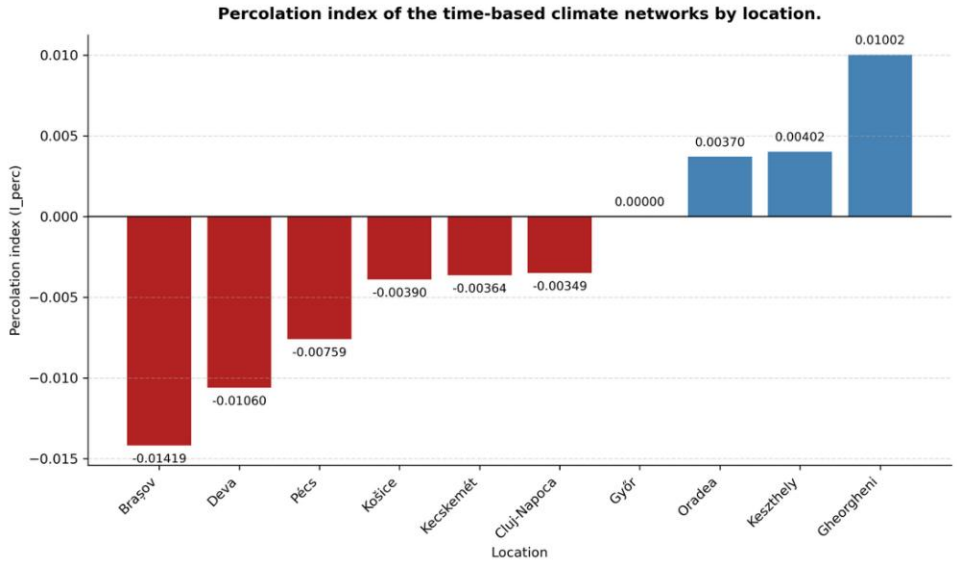


**Fig. 8.** Percolation index by location.

A second group includes location where the index was zero, in our case Győr. In this case, the late-period network remained connected up to a slightly higher similarity threshold. This shows that local or monthly reorganisation does not necessarily mean that the full network becomes weaker. A network can become more internally differentiated while its strongest connections remain stable or even slightly stronger.

The third group consists of locations where the percolation index presents positive values: Gheorgheni, Oradea and Keszthely. At these sites, the percolation curves suggest that a local gain in structural robustness is present.

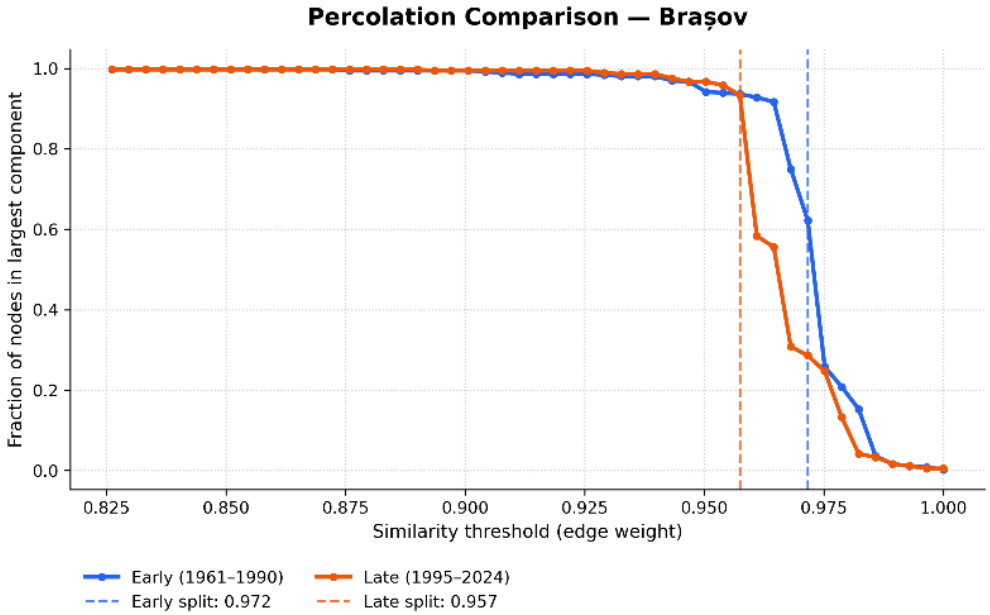


**Fig. 9.** Percolation Comparison for Brasov

## 5. DISCUSSION

The time-based climate network analysis demonstrates that recent climate change in the Carpathian Basin manifests not merely as a shift in isolated variables, but as a systemic structural reconfiguration of seasonality. The preservation of the core winter and summer communities across all ten locations indicates that the macro-level, seasonal cycle remains fundamentally intact. However, the universal decrease in network modularity reveals that the boundaries separating these seasonal blocks have become less distinct in the contemporary period. Rather than a collapse of the annual cycle or a simple increase in climate volatility, these findings point toward a highly organized, location-specific redistribution of climatic similarity, concentrated primarily at the margins of the traditional seasons.

The most coherent basin-wide signal emerges during the late winter and early spring transition, characterized by an asymmetry between February and March. In the historical baseline period, March was characterized by elevated Shannon entropy, acting as a volatile, fragmented bridge between winter-like and spring-like states. In the recent period, March has stabilized into a more consistent, coherent transitional position. Concurrently, February has experienced a profound surge in fragmentation across nine of the ten studied locations. This macro-regional inversion suggests a structural phase advancement in the onset of spring-like conditions, a phenomenon that echoes the large-scale seasonal changes observed across Europe by Stine et al. (2009). Late winter is no longer consistently anchored to the core cold-season regime; instead, it frequently fluctuates toward warmer, transitional states. This increased structural ambiguity in February matches the empirical findings of Spinoni et al. (2015a), who identified a significant increase in late-winter thermal extremes and shifting heat/cold wave frequencies within the Carpathian region.

Beyond the late-winter shift, the transitions of mid-spring (April) and autumn (September to November) reveal high spatial heterogeneity. The network indicators do not show a uniform basin-wide trend; instead, northwestern and lowland plain locations exhibit increased fragmentation during these shoulder months, whereas southeastern foothill sites and sheltered intra-mountain depressions show stable or even decreasing entropy. This localized divergence underscores the critical role of topographic controls in modulating regional climate change impacts, as highlighted by Spinoni et al. (2015b). The open, lowland landscapes of the Pannonian Basin are highly susceptible to shifting advective regimes and moisture fluctuations, leading to highly variable transitional states. Conversely, the weaker or more spatially variable changes observed at mountain-influenced locations may be partly related to topographic control, but this interpretation remains tentative. E-OBS represents grid-cell-scale climatic conditions and may smooth elevation gradients, valley inversions, cold-air pooling and local orographic precipitation. The apparent contrast between lowland and mountain-influenced sites should therefore be interpreted as a regional grid-scale pattern rather than as direct evidence of local microclimatic buffering. These complex local responses confirm that broad geographical generalizations are insufficient for tracking seasonal architecture, aligning with the highly localized variations in regional climate indices modelled by Megyeri-Korotaj et al. (2023).

The prototype similarity matrices provide a direct look into the nature of this structural mixing, uncovering off-diagonal relationships between entirely different parts of the annual cycle. The high multi-dimensional similarity observed between early spring (April/May) and mid-to-late autumn (September/October) indicates that the climatic profiles of these shoulder periods are increasingly overlapping. This cross-seasonal convergence suggests a flattening of the transition gradients within the basin. As shoulder seasons expand and increasingly mimic one another, the distinct meteorological identities of spring and autumn become blurred. This systemic blending of transitional states could have important implications for regional water cycles, agricultural growing windows, and environmental stability, corroborating the compounding hydrological tendencies discussed by Bartholy and Pongrácz (2007) and Jánosi et al. (2023). The percolation analysis qualifies these findings by demonstrating that this internal restructuring did not cause a major degradation of global network connectivity. The mean percolation index remained close to zero across the basin, with subtle localized shifts toward fragility or robustness depending on the site's physiographic setting. This behaviour shows that a climate network can experience enhanced internal overlap and weaker

community boundaries at its boundaries while maintaining the absolute stability of its core structural backbone.

From a methodological perspective, adapting a temporal-node framework to climate networks provides a valuable complement to conventional trend and anomaly analyses. Traditional grid-cell networks excel at highlighting spatial teleconnections and regional coupling, but they obscure the internal structural relationships between temporal states. By treating individual month-year observations as distinct multidimensional vectors, this approach successfully captures changes in the systemic architecture of seasonality that are invisible when variables are analysed in isolation.

Three methodological settings are relevant when considering the robustness of the analysis: the number of retained PCA components, the target average degree used for network pruning, and the resolution parameter of the Leiden community-detection algorithm. These settings were defined prior to the comparison and were applied identically to all locations and both periods. The retention of two principal components was supported by the high cumulative proportion of variance explained by the first two components, which ranged from 91.5% (Gheorgheni) to 93.7% (Kecskemét) across the ten locations. The two-dimensional PCA representation therefore preserved the dominant structure of the six climatic variables, while also providing a consistent and parsimonious similarity space. The use of additional components would introduce only a comparatively limited amount of residual variance and would reduce the interpretability of the common distance space.

The target average degree was likewise not selected as an arbitrary tuning parameter, but was derived analytically from the expected seasonal neighbourhood of each node. In a 30-year period, each year–month observation can be associated with the other 29 occurrences of the same calendar month and with the 30 occurrences of each adjacent month, resulting in a target average degree of $29 + 30 + 30 = 89$. Changing this value would therefore imply a different assumption about the temporal extent of the seasonal neighbourhood rather than a minor adjustment of network density. Finally, the Leiden resolution parameter was set to its standard value of 1.0, corresponding to the conventional weighted-modularity formulation. It was not optimised separately by location or period, thereby avoiding a posteriori adjustment of community granularity. Although alternative resolution values may affect the exact number or boundaries of detected communities, the use of a common standard setting, together with the recurrence of the main patterns across locations and across complementary indicators, supports the internal consistency of the comparison. This does not imply complete parameter invariance, but it reduces the likelihood that the principal conclusions are artefacts of location- or period-specific parameter tuning.

Several limitations must be considered when interpreting these outcomes. The analysed E-OBS values are spatially interpolated grid-cell estimates rather than direct observations at the selected cities. Interpolation uncertainty varies with station density and may also change through time as the underlying observational network changes. Previous evaluations have shown that gridded estimates are generally less reliable for spatially heterogeneous variables, particularly precipitation, and in regions characterised by sparse observations or complex terrain (Hofstra et al., 2009; Cornes et al., 2018). At the 0.1° grid scale, local elevation contrasts, slope exposure, valley inversions, cold-air pooling and fine-scale orographic precipitation cannot be fully represented. This limitation is particularly relevant for Gheorgheni and Brașov and, to a lesser extent, for the other foothill and basin locations. Consequently, the location-specific results should be interpreted as regional grid-cell-scale signals rather than as exact descriptions of urban or valley-floor microclimates. Monthly aggregation and the consistent use of the same grid cells in both periods may reduce the influence of short-term random interpolation errors, but they do not eliminate systematic topographic smoothing, temporal changes in station density or possible inhomogeneities in the input observations.

Because the analysis parameters were held strictly constant across both analysis intervals, the comparative validity between the periods remains robust. However, the 30-year snapshot comparison is inherently static; it identifies clear structural differences between the two blocks but cannot trace the exact timing, velocity, or continuity of the transition. Integrating moving-window network formulations and comprehensive sensitivity testing represents a highly promising avenue for future extensions of this research.

## 6. CONCLUSIONS

This study used a time-based climate-network approach to compare the seasonal organisation of climate in the Carpathian Basin during 1961–1990 and 1995–2024. The annual cycle remained recognisable in the later period: winter and summer cores persisted, while seasonal communities became less clearly separated at all ten locations.

The strongest reorganisation affected transition months. February became more fragmented at nine locations, whereas March became more coherent everywhere. April showed increased fragmentation at Győr, Košice, Cluj-Napoca and Deva, but decreases at Kecskemét, Pécs and Brașov. October became more fragmented at Győr, Kecskemét, Keszthely and Oradea, while Košice and Brașov showed decreases. September remained a persistent boundary month, and at Pécs strong off-diagonal prototype similarities confirmed greater overlap between spring and autumn climatic states.

Percolation results indicate that these changes did not produce a general loss of network robustness. Brașov and Deva showed the clearest weakening, with smaller negative shifts at Pécs, Košice, Kecskemét and Cluj-Napoca. Győr remained essentially unchanged, whereas Gheorgheni, Oradea and Keszthely showed modest gains. The findings indicate a moderate reorganisation rather than a collapse of seasonality. Climate change altered the relationships between monthly climatic states mainly at seasonal boundaries, while the core annual structure remained intact. Time-based climate networks therefore complement conventional trend analysis by revealing structural changes not captured by individual climatic variables alone.

## REFERENCES

Bartholy, J. and Pongrácz, R. (2007) ‘Regional analysis of extreme temperature and precipitation indices for the Carpathian Basin from 1946 to 2001’, *Global and Planetary Change*, 57(1–2), pp. 83–95. doi: 10.1016/j.gloplacha.2006.11.002.

Donges, J.F., Zou, Y., Marwan, N. and Kurths, J. (2009) ‘Complex networks in climate dynamics’, *The European Physical Journal Special Topics*, 174, pp. 157–179. doi: 10.1140/epjst/e2009-01098-2.

Fan, J., Meng, J., Ashkenazy, Y., Havlin, S. and Schellnhuber, H.J. (2018) ‘Climate network percolation reveals the expansion and weakening of the tropical component under global warming’, *Proceedings of the National Academy of Sciences of the United States of America,* 115(52), pp. E12128–E12134. doi: 10.1073/pnas.1811068115.

Hajek, O.L. and Knapp, A.K. (2022) ‘Shifting seasonal patterns of water availability: ecosystem responses to an unappreciated dimension of climate change’, *New Phytologist,* 233(1), pp. 119–125. doi: 10.1111/nph.17728.

Holme, P. and Rocha, J.C. (2023) ‘Networks of climate change: connecting causes and consequences’, *Applied Network Science,* 8(1), article 10, pp. 1–20. doi: 10.1007/s41109-023-00536-9.

Holme, P. and Saramäki, J. (2012) ‘Temporal networks’, *Physics Reports,* 519(3), pp. 97–125. doi: 10.1016/j.physrep.2012.03.001.

Jánosi, I.M., Bíró, T., Lakatos, B.O., Gallas, J.A.C. and Szöllősi-Nagy, A. (2023) ‘Changing water cycle under a warming climate: Tendencies in the Carpathian Basin’, *Climate,* 11(6), article 118. doi: 10.3390/cli11060118.

Ludescher, J., Bunde, A. and Schellnhuber, H.J. (2023) ‘Forecasting the El Niño type well before the spring predictability barrier’, *npj Climate and Atmospheric Science,* 6, article 196. doi: 10.1038/s41612-023-00519-8.

Megyeri-Korotaj, O.A., Bán, B., Suga, R., Allaga-Zsebeházi, G. and Szépszó, G. (2023) ‘Assessment of climate indices over the Carpathian Basin based on ALADIN5.2 and REMO2015 regional climate model simulations’, *Atmosphere,* 14(3), article 448. doi: 10.3390/atmos14030448.

Mucha, P.J., Richardson, T., Macon, K., Porter, M.A. and Onnela, J.-P. (2010) ‘Community structure in time-dependent, multiscale, and multiplex networks’, *Science,* 328(5980), pp. 876–878. doi: 10.1126/science.1184819.

Newman, M.E.J. (2006) 'Modularity and community structure in networks', *Proceedings of the National Academy of Sciences of the United States of America,* 103(23), pp. 8577–8582. doi: 10.1073/pnas.0601602103.

Shannon, C.E. (1948) 'A mathematical theory of communication', *The Bell System Technical Journal,* 27(3), pp. 379–423, 623-656. doi: 10.1002/j.1538-7305.1948.tb01338.x.

Spinoni, J., Lakatos, M., Szentimrey, T., Bihari, Z., Szalai, S., Vogt, J. and Antofie, T. (2015a) 'Heat and cold waves trends in the Carpathian Region from 1961 to 2010', *International Journal of Climatology,* 35(14), pp. 4197–4209. doi: 10.1002/joc.4279.

Spinoni, J., Szalai, S., Szentimrey, T., Lakatos, M., Bihari, Z., Nagy, A., Németh, Á., Kovács, T., Mihic, D., Dacic, M., Petrovic, P., Kržič, A., Hiebl, J., Auer, I., Milkovic, J., Štepánek, P., Zahradníček, P., Kilar, P., Limanowka, D., Pyrc, R., Cheval, S., Birsan, M.-V., Dumitrescu, A., Deak, G., Matei, M., Antolovic, I., Nejedlik, P., Štastný, P., Kajaba, P., Bochníček, O., Galo, D., Mikulová, K., Nabyvanets, Y., Skrynyk, O., Krakovska, S., Gnatiuk, N., Tolasz, R., Antofie, T. and Vogt, J. (2015b) 'Climate of the Carpathian Region in the period 1961–2010: climatologies and trends of 10 variables', *International Journal of Climatology,* 35(7), pp. 1322–1341. doi: 10.1002/joc.4059.

Stine, A.R., Huybers, P. and Fung, I.Y. (2009) 'Changes in the phase of the annual cycle of surface temperature', *Nature*, 457, pp. 435–440. doi: 10.1038/nature07675.

Stine, A.R. and Huybers, P. (2012) 'Changes in the seasonal cycle of temperature and atmospheric circulation', *Journal of Climate*, 25(21), pp. 7362–7380. doi: 10.1175/JCLI-D-11-00470.1.

Traag, V.A., Waltman, L. and van Eck, N.J. (2019) 'From Louvain to Leiden: guaranteeing well-connected communities', *Scientific Reports,* 9, article 5233. doi: 10.1038/s41598-019-41695-z.

Tsonis, A.A. and Roebber, P.J. (2004) 'The architecture of the climate network', *Physica A: Statistical Mechanics and its Applications,* 333, pp. 497–504. doi: 10.1016/j.physa.2003.10.045.

Tsonis, A.A., Swanson, K.L. and Roebber, P.J. (2006) 'What do networks have to do with climate?', *Bulletin of the American Meteorological Society,* 87(5), pp. 585–596. doi: 10.1175/BAMS-87-5-585.